

Analysis of Crossover Between Local and Massive Separation on Airfoils

Mark Barnett*

United Technologies Research Center, East Hartford, Connecticut

The occurrence of massive separation on airfoils operating at high Reynolds number poses an important problem to the aerodynamicist. In the present study, the phenomenon of crossover, induced by airfoil thickness, between local separation and massive separation is investigated for low-speed (incompressible) symmetric flow past realistic airfoil geometries. This problem is studied both for the infinite Reynolds number asymptotic limit using triple-deck theory and for finite Reynolds number using interacting boundary-layer theory. Numerical results are presented that illustrate how the flow evolves from local to massive separation as the airfoil thickness is increased. The results of the triple-deck and the interacting boundary-layer analyses are found to be in qualitative agreement for the NACA four-digit series and an uncambered supercritical airfoil. The effect of turbulence on the evolution of the flow is also considered. Solutions are presented for turbulent flows past a NACA 0014 airfoil and a circular cylinder. For the latter case, the calculated surface pressure distribution is found to agree well with experimental data if the proper eddy pressure level is specified.

Introduction

THE present effort focuses on the phenomenon of thickness-induced massive separation for airfoils in steady, symmetric, incompressible flow by analyzing the "crossover" process; i.e., the process by which a flow with small-scale local separation evolves into one with massive separation as airfoil thickness is increased. The understanding gained through consideration of thickness-induced stall will be helpful in understanding massive separation induced by loading. Restricting the analysis to steady flow eliminates the need to predict the complex unsteady development of the massive separation structure that may arise.

An understanding of the phenomenon of massive separation is important, since its onset generally corresponds to the limit of the effective range of operation of an airfoil. Beyond a simple reduction in efficiency, massive separation (stall) can lead to conditions that compromise the safe operation of an aircraft. One example is the phenomenon of tip stall, where locally stalled flow occurs near one of the wingtips. The associated loss of lift generates a large rolling moment on the vehicle, which can induce a hazardous spin. In turbomachines, blade stall can lead to a reduction in efficiency and, in the worst case, a loss of power. In addition, with the recent interest in highly maneuverable aircraft designed to fly at or near stalled conditions, an understanding of the massive separation phenomenon becomes increasingly important for the efficient design of such vehicles.

The analyses employed herein rely on the assumption that boundary-layer theory applies, in many cases, up to and beyond the initial onset of massive separation; this is supported by a number of theoretical studies.¹⁻³ Relatively simple models for the analysis of massive separation on airfoils have resulted from the boundary-layer assumption. The knowledge gained from these models can be used to assist in the development of algorithms relying upon the Navier-Stokes equations to represent the stall phenomenon.

Two theoretical approaches are employed in this study. It is assumed in both that the massive separation bubble is a region of constant pressure, i.e., that it is a Kirchhoff eddy, which permits the use of the generalized Cheng-Rott⁴ thin-airfoil theory to model the inviscid flow. The two approaches differ in the way the viscous flow is treated. In the first method, the problem is viewed in the infinite Reynolds number (Re) asymptotic limit by utilizing triple-deck theory, wherein viscous effects are significant only in the immediate neighborhood of the separation point. This results in the so-called Sychev-Smith^{1,2} model for massive separation. The second approach allows for finite Reynolds number effects by using interacting boundary-layer theory, where the boundary-layer equations are solved from the leading-edge stagnation point to a location downstream of separation. The interacting boundary-layer procedure employed herein to calculate massively separated flows is based upon that developed by Rothmayer and Davis,⁵ who calculated massive separation on a model airfoil geometry. In addition, finite Reynolds number small-scale local separation is also calculated here using an interacting boundary-layer analysis in conjunction with the usual form of the incompressible thin-airfoil integral equation to represent the inviscid flow. Triple-deck and interacting boundary-layer calculations are performed for two different families of symmetric airfoils, namely the NACA four-digit series airfoil and an uncambered supercritical airfoil, for which the airfoil thickness is systematically varied in order to investigate the crossover process.

The Kirchhoff eddy model used herein does not address the issue of closure of the massive eddy, but instead assumes that the eddy grows parabolically and is open at downstream infinity. Although the correct behavior of the flow on the local (body) scale is believed to be properly captured by the present model, the issue of eddy closure is a very important one to consider in the development of a *comprehensive* model of stall. A number of articles exploring the eddy closure problem have been published by Smith^{2,3,6,7} and, although no complete description of eddy closure currently exists, they provide much insight into the complexity and the current level of understanding of the problem.

The methods of analysis employed herein are shown to be very useful for predicting the crossover behavior occurring for realistic airfoils. In particular, the behaviors predicted by the triple-deck and interacting boundary-layer analyses are in

Received May 26, 1987; revision received Jan. 27, 1988. Copyright © American Institute of Aeronautics and Astronautics, Inc., 1988. All rights reserved.

*Research Engineer. Member AIAA.

qualitative agreement for the airfoils considered. The present interacting boundary-layer analysis has also been used to investigate the effects of turbulence on separated flow and the crossover process. Interacting boundary-layer theory is shown to be an efficient tool for the analysis of the crossover between local and massive separation on airfoils.

Problem Description and Formulation

The two theories applied in this study, namely, triple-deck and interacting boundary-layer theory, are described in the following sections. In the discussion that follows, distances are normalized by a characteristic length scale L , taken here to be the airfoil chord, the pressure is normalized by twice the freestream dynamic pressure ρU_∞^2 , and viscosity is nondimensionalized by its freestream value μ_∞ .

Triple-Deck Theory

One of the goals of the present investigation is to be able to determine how the extent of the separated flow region varies as a function of airfoil thickness for realistic airfoils. In order to accomplish this, the asymptotic behavior (for $Re \rightarrow \infty$) of the separation point location has been calculated using the triple-deck analysis, which was presented in Ref. 8 and is briefly reviewed now.

In the triple-deck analysis, two fundamental assumptions are made regarding the structure of a massively separated flow. The first is that the eddy that arises downstream of the boundary-layer breakaway point contains a weak recirculating current, and therefore the pressure is constant throughout the eddy. This model is consistent with Kirchhoff's⁹ free-streamline theory, which assumes that the eddy does not close but instead grows parabolically downstream of separation. The second assumption follows that adopted by Sychev,¹ whereby separation is assumed to occur within a triple-deck structure. Consistent with this, the behavior of the pressure in the region just upstream of the separation point is of the form

$$p - p_e \sim -\alpha \lambda^{9/8} \epsilon^{1/2} (x_o - x)^{1/2}, \quad x \rightarrow x_o^- \quad (1)$$

where x is the arc length measured along the surface from the stagnation point, x_o is the separation point location ($0 < x_o < 1$), p is the surface pressure, p_e is the (constant) pressure within the eddy downstream of separation, λ is the wall shear at $x = x_o$, which is evaluated using classical (weak-interaction) boundary-layer theory, α is the positive constant determined by Smith² to have the value 0.44, and

$$\epsilon = Re^{-1/8} = \left(\frac{\rho U_\infty L}{\mu} \right)^{-1/8} \quad (2)$$

therefore $\epsilon \rightarrow 0$ as $Re \rightarrow \infty$. The form of Eq. (1) was determined by simultaneously satisfying the local requirements of both the viscous and inviscid flows in the vicinity of separation.¹ The boundary layer must separate in an adverse pressure gradient, and since the only existing *nonsingular* inviscid free-streamline (potential) theory solution has a *zero* pressure gradient at separation,² the surface pressure distribution for the inviscid flow must be singular at the separation point. The increasingly adverse pressure gradient given by Eq. (1) is exactly consistent with the requirements of triple-deck viscous separation, and in turn, triple-deck theory provides a mechanism to smooth the singularity in the inviscid pressure distribution as the flow passes through separation. Therefore, Eq. (1) represents the criterion for the pressure at a laminar separation point for massively separated flow.

The triple-deck analysis is based on the assumption that thin-airfoil theory can be used to model the inviscid flow on the body scale [$x = O(1)$]. The coordinate system employed has its origin at the airfoil leading edge, with the x axis oriented along the chord line, x increasing in the downstream direction, the y axis normal to the oncoming uniform flow, and y

increasing in the upward direction. Upstream of the separation point at x_o , the body shape is known and is written in the form $y = Re^{-1/16} \tilde{h} f(x)$, where the function $f(x)$ represents the body profile and \tilde{h} is the $O(1)$ airfoil thickness parameter, so that the physical airfoil thickness is $O(Re^{-1/16})$.

Downstream of the location $x = x_o$, a Kirchhoff constant pressure eddy is assumed to exist, within which the pressure is equal to the freestream pressure; i.e., $p_e = 0$ in Eq. (1). The assumption of a constant pressure eddy, along with the use of thin-airfoil theory, implies that upstream of x_o the normal velocity can be specified along the x axis, whereas downstream of the separation point a constant value of the tangential velocity can be specified. Therefore, the resulting thin-airfoil problem is one of mixed boundary-value type. The surface pressure is given by the elliptic integral equation⁴

$$\tilde{p}(x, 0) = -\frac{\tilde{h}}{\pi} (x_o - x)^{1/2} \int_0^{x_o} \frac{f'(s)}{(x_o - s)^{1/2} (x - s)} ds, \quad x < x_o \quad (3)$$

where $\tilde{p} = Re^{1/16} p \sim O(1)$ and p is the nondimensional physical pressure.

After applying the triple-deck criterion for the pressure at the separation point, Eq. (1), to Eq. (3), the following condition for determining the location of the separation point x_o , is obtained:

$$\int_0^{x_o} \frac{f'(s)}{(x_o - s)^{3/2}} ds = \frac{\alpha \lambda^{9/8} \pi}{x_o^{9/16} \tilde{h}} \quad (4)$$

Thus, the triple-deck problem for massive separation requires the solution of a single integral equation, Eq. (4), and distills from a very complicated physical problem a relatively simple mathematical statement that contains the essential features of the original problem. In the present study, the airfoil profiles $f(x)$ are specified in analytical form, allowing Eq. (4) to be solved exactly. Solutions of Eq. (4) are conveniently determined by solving the inverse problem to determine \tilde{h} as a function of x_o .

The inviscid flow representation used in the foregoing massive separation model predicts parabolic growth of the eddy far downstream, i.e., $S(x) \sim bx^{1/2}$ where $S(x)$ is the free-streamline shape and b is a measure of the growth rate. The coefficient b is obtained as part of the solution of the triple-deck problem. Parabolic growth of the eddy in the farfield downstream flow is consistent with the Kirchhoff eddy model; thus, the Cheng-Rott integral recovers the correct downstream boundary condition. If $b > 0$, the eddy thickness grows with increasing distance downstream, while if $b < 0$, the free streamlines cross the symmetry or x axis at a finite distance downstream of the airfoil. The latter situation is not physically plausible. There is generally a value of $x_o < 1$ for which $b = 0$, which has special significance. This value of x_o corresponds to the phenomenon referred to as "cutoff."⁸ If the airfoil thickness is decreased below the cutoff value, an entirely new flow structure arises wherein the eddy dimensions are considerably diminished compared to its dimensions prior to cutoff.

A number of very interesting and significant results have emerged from the triple-deck analysis carried out by Cheng and Smith.⁸ One result of particular interest here concerns the effect of airfoil trailing-edge geometry on the way crossover occurs. The crossover process for airfoils with wedge-shaped trailing edges can be significantly different than that for cusped trailing-edge airfoils. In the former case, the crossover between local and massive separation is found to be continuous as the airfoil thickness parameter \tilde{h} is varied. That is, the growth or collapse of the separated region occurs smoothly as \tilde{h} is varied, and each value of \tilde{h} determines a unique flow state. In contrast, it has been shown⁸ that, for airfoils with cusped trailing edges, multiple flow states (nonuniqueness) can exist for some values of \tilde{h} . Furthermore, the crossover process for such airfoils is quite possibly an unsteady phenomenon.

Another important result of the analysis in Ref. 8 is the discovery of a possible mechanism for the phenomenon of stall hysteresis, which has been observed experimentally for quite some time. Finally, Rothmayer¹⁰ points out that non-uniqueness can arise under a more general condition than that determined in Ref. 8, where the presence of a cusped trailing edge was found to be the controlling factor—the existence of an inflection point in the airfoil geometry can induce non-uniqueness, even if the trailing edge is wedge-shaped.

Interacting Boundary-Layer Theory

High-Reynolds number flow past an airfoil is characterized by a weak interaction between the viscous displacement thickness and the inviscid flow over most of the airfoil surface, with local regions of strong viscous/inviscid interaction existing, e.g., in the vicinity of the trailing edge or at a separation point. In the described triple-deck analysis of massive separation, viscous effects are confined to the immediate neighborhood of the separation point; there is no contribution from weak interaction effects. In contrast, at finite Reynolds number it is necessary to account for the global effect of the displacement thickness along the entire airfoil and the wake, in addition to the contribution from local strong interactions, to properly predict the flowfield. Therefore, in the interacting boundary-layer approach, it is necessary to consider the effect of the viscous-layer thickness distribution over the semi-infinite domain spanned by the airfoil and its wake. The use of the Kirchhoff eddy model for massive separation permits the streamwise extent of the calculation domain to be reduced to a finite length less than the airfoil chord, thus contributing significantly to the efficiency of this technique. It is important to note that both the elliptic nature of the inviscid flow and the parabolic growth of the massive eddy in the downstream farfield are reflected in this massive separation model, which is derived based on the assumption of a semi-infinite constant pressure region aft of the separation point.

Viscous Flow

The governing equations for the viscous flow are the boundary-layer equations. In the present study, the incompressible boundary-layer equations are written in a coordinate system that is located within the shear layer but a small distance from the body surface or wake centerline. This "shear layer" or "baseline" coordinate system was introduced by Werle and Verdon,¹¹ and its principal use is to permit better alignment of the boundary-layer coordinate system with the shear layer than can be obtained with a body-oriented coordinate system.

In order to provide more efficient and potentially more accurate solutions to the boundary-layer equations, similarity-type variables are introduced. Because they take advantage of the locally similar nature of the flow, their use minimizes streamwise gradients. In addition, similarity variables account for the growth of a laminar boundary-layer, thereby allowing the use of a fixed number of grid points in the normal direction. A modified form of the Görtler variables are used and are given by

$$\xi = \int_0^s U_{e_o}(t) dt \quad (5a)$$

and

$$\eta = \frac{U_{e_o}(s)}{\sqrt{2\xi}} n \quad (5b)$$

where s is the arc length measured from the leading edge along the baseline curve and U_{e_o} is the inviscid tangential velocity at the baseline coordinate surface. Letting u and v represent the velocity components in the local surface tangential and normal

directions, respectively, transformed similarity velocity functions F and V are defined as follows:

$$u = U_{e_o} F \quad (6)$$

and

$$v = \frac{U_{e_o}}{\sqrt{2\xi}} V - \frac{\partial \eta}{\partial s} \sqrt{2\xi} F \quad (7)$$

The continuity and momentum equations in transformed variables become

$$V_\eta + F + 2\xi F_\xi = 0 \quad (8)$$

and

$$(\bar{\epsilon} F_\eta)_\eta - V F_\eta + F V_\eta + \beta_1 + (1 - \beta_o) F^2 = 0 \quad (9)$$

respectively, where β_o and β_1 are defined by

$$\beta_o = \frac{2\xi}{U_{e_o}} \frac{dU_{e_o}}{d\xi} \quad (10)$$

and

$$\beta_1 = \frac{2\xi}{U_{e_o}^2} U_e \frac{dU_e}{d\xi} \quad (11)$$

The quantity β_o is the pressure gradient parameter for the inviscid flow over the baseline coordinate surface, β_1 is the pressure gradient parameter for the interacted flow, and U_e is the inviscid surface speed for flow past the "effective" body, i.e., the body thickened by the viscous displacement effect. The momentum equation has been written in a general form that allows for the introduction of turbulence effects through the term $\bar{\epsilon} = 1 + \epsilon$. Here, ϵ is the turbulent eddy-viscosity coefficient,¹² which is set to zero for laminar flow. A modified form of the Cebeci-Smith¹³ turbulence model is utilized for surface boundary layers, and the turbulence model of Chang et al.¹⁴ is applied for turbulent wakes.

The boundary conditions must also be transformed into similarity variables. The solid surface boundary conditions become

$$F(\xi, 0) = 0 \quad (12a)$$

and

$$V(\xi, 0) = 0 \quad (12b)$$

The wake centerline boundary conditions are

$$\frac{\partial F}{\partial \eta}(\xi, 0) = 0 \quad (12c)$$

and

$$V(\xi, 0) = 0 \quad (12d)$$

The edge conditions become

$$F - U_e/U_{e_o}, \quad \eta \rightarrow \eta_{\max} \quad (13)$$

and

$$V - \eta V_\eta - \sqrt{2\xi} \frac{d}{d\xi} (U_e \delta^*), \quad \eta \rightarrow \eta_{\max} \quad (14)$$

The latter conditions arise from matching the viscous and the inviscid tangential and normal velocities at the edge of the viscous layer. Finally, the displacement thickness δ^* is given

by

$$\delta^* = \frac{\sqrt{2\xi}}{U_{e_0}} \int_0^\infty \left(1 - \frac{U_{e_0}}{U_e} F\right) d\eta \quad (15)$$

Inviscid Flow

The inviscid flow is modeled by assuming that thin-airfoil theory is applicable. Two inviscid models are needed, the first for application to attached flows or flows with relatively small separation bubbles, and the second for flows in which massive separation occurs. These models will be referred to as the Local Strong-Interaction (LSI) model and the Massive Separation (MS) model, respectively.

In the LSI model, classical thin-airfoil theory for incompressible flow is employed. In this theory, the displacement body is represented by normal injection through the baseline coordinate surface. The injection velocity distribution is related to the inviscid tangential velocity at the edge of the boundary layer through the Cauchy principal-value integral (e.g., see Ashley and Landahl¹⁵):

$$U_e(x) = U_{e_0}(x) \left(1 + \frac{1}{\pi} \oint_0^\infty \frac{W(t, 0)}{x-t} dt\right) \quad (16)$$

Here, W is the normal injection velocity at the airfoil surface, i.e.,

$$W(x, 0) = \frac{1}{\sqrt{Re}} \frac{d}{dx} [U_e(\delta^* + f)] \quad (17)$$

where f is the normal distance from the baseline coordinate surface (positive in the direction of the outward normal). Note that in most applications of thin-airfoil theory, the baseline coordinate surface is chosen to be the x axis, for which the inviscid tangential velocity along the baseline surface $U_{e_0} = 1$.

In the MS model, the inviscid flow is divided into two regions. The first extends from the leading edge to a specified point on the airfoil surface at $x = x_e$ ($0 < x_e < 1$), within which the displacement body is to be calculated. The second, where $x \geq x_e$, is assumed to be a region of (specified) constant pressure. Since x_e is in the constant-pressure region, its value must be chosen such that the separation point is upstream of x_e or a massive separation solution will not be obtained. In the upstream and downstream regions, the displacement body is represented by normal injection and the constant pressure is represented by a constant tangential velocity, respectively. The generalized method for mixed boundary-value problems in thin-airfoil theory, developed in Ref. 4, was applied to the massive separation problem by Rothmayer and Davis⁵ to obtain the integral

$$U_e(x) = U_{e_0}(x) \left[1 + \frac{\sqrt{x_e - x}}{\pi} \oint_0^{x_e} \frac{W(t, 0)}{(x-t)\sqrt{x_e - t}} dt + I_e(x) \right], \quad x < x_e \quad (18)$$

where the term I_e has been introduced to account for the possibility that the tangential velocity of the inviscid flow past the baseline coordinate surface has not reached the freestream value when $x = x_e$, and is given in Ref. 10. This term is also used to specify the desired value of the eddy pressure. It should be noted that the massive separation of the Interacting Boundary Layer (IBL) calculation is carried out in the finite region from $x = 0$ to $x = x_e$, which in general is a smaller domain than that required for the LSI approach, for which the calculation region extends into the wake.

Because most real airfoils have blunt leading edges, thin-airfoil theory cannot be applied in its usual form, since this theory is invalid near a blunt leading edge. To overcome this limitation, instead of regarding the flow as a small perturbation to a uniform stream (i.e., flow past a flat plate),

the flow past a blunt-nosed airfoil is represented as a small perturbation to the flow past the parabola having the same nose radius as the airfoil under consideration, i.e., the "osculating" parabola. Therefore, the osculating parabola is chosen as the baseline coordinate curve. The inviscid flow past a parabola can be solved analytically using conformal mapping to map the parabola to a stagnation plane. In the present study, the parabolic baseline coordinate surface is used for both the LSI and the MS calculations to permit the use of thin-airfoil theory for calculations of symmetric flow past blunt-nosed airfoils.

Numerical Method

The triple-deck massive separation problem can be solved analytically. In contrast, a numerical analysis is required for the nonlinear partial differential equations governing the interacting boundary-layer problem. A finite-difference approach is used to solve the viscous-layer equations, and the same technique applies to both the local strong interaction and the massive separation problem. The appropriate inviscid governing equation, either the Cauchy integral [Eq. (16)] or the Cheng-Rott integral [Eq. (18)] for the local strong interaction and the massive separation problems, respectively, is solved after discretization.

The key feature of the IBL approach is its ability to account for strong interactions between the viscous and the inviscid regions of the flow, which are driven by the viscous displacement effect. Therefore, an important consideration in the development of a numerical technique for the analysis of the interacting boundary-layer equations is the method used to couple the solutions of the viscous and the inviscid equations, since the strong mutual interaction that can exist between the two is reflected principally in the coupling. The technique used here is the quasimultaneous coupling procedure introduced by Veldman¹⁶ and Davis and Werle.¹⁷

A general form for the discretized inviscid integral, either Eq. (16) or Eq. (18), is given by

$$U_{e_i} = \bar{g}_i + \frac{1}{\pi} \sum_{j=1}^{IE} T_j D_{ij} + \frac{1}{\pi} (U_e \delta^*)_i D_{ii} \quad (19a)$$

where i denotes the index in the marching or x direction; i.e., the solution is sought at $x = x_i$. Here, IE is the index of the farthest downstream station in the solution domain, and D_{ij} represents the "influence coefficients" arising from the discretization of the inviscid equations. Equation (19a) can be written in the compact form

$$U_{e_i} = \bar{C}_i + \bar{D}_i (U_e \delta^*)_i \quad (19b)$$

which gives an explicit relationship between U_e and δ^* at x_i . The coupling of the viscous and inviscid equations is accomplished by utilizing Eq. (19b), obtained from the governing inviscid equation, and Eq. (14), the viscous boundary condition on the normal velocity at the viscous-layer edge, to simultaneously solve for U_{e_i} and δ^*_i . For a more detailed description of the coupling procedure and the definitions of the coefficients of the discretized inviscid equations, the reader is referred to Ref. 12.

The complete viscous/inviscid interaction solution is determined by globally iterating upon the displacement thickness distribution starting with an initial guess. Each spatial sweep of the boundary-layer equations is handled in a parabolic-like manner, marching the equations from an initial boundary-layer profile, which is generally a similarity profile. During each spatial sweep of Eq. (19a), the update of δ^* is treated in Gauss-Seidel fashion using the latest available values; i.e., δ^* is known at the current global iteration level for $j < i$ and at the previous iteration level for $j > i$ and is unknown at $j = i$. Convergence of the calculation is determined by monitoring the maximum fractional change in the displacement thickness from one global iteration to the next until it falls below some

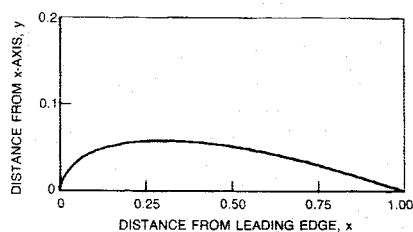


Fig. 1a NACA 0012 airfoil thickness profile.

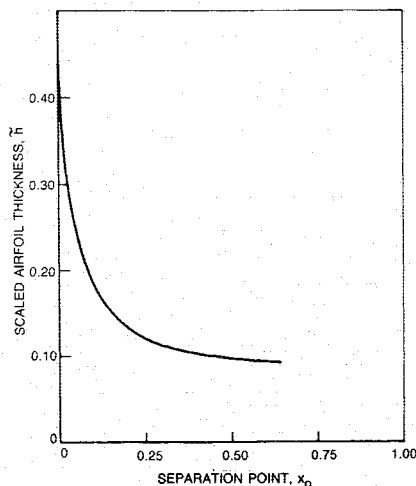


Fig. 1b Asymptotic behavior of separation point location for NACA 00XX airfoil.

preset tolerance, usually 10^{-5} , at which point the calculation is terminated.

Discussion of Results

The analyses discussed have been applied to two families of realistic symmetric airfoils, namely the NACA four-digit series airfoil, NACA 00XX, where XX represents the maximum thickness of the airfoil expressed in percent of chord, and the family of uncambered airfoils generated from the thickness distribution of the Garabedian and Korn (GK) supercritical airfoil with the designation 70-10-13.¹⁸ The thickness function $f(x)$ of the former airfoil is given by an analytical expression of the form

$$f(x) = a_0 x^{1/2} + a_1 x + a_2 x^2 + a_3 x^3 + a_4 x^4 \quad (20)$$

The original coefficients for this airfoil are given in Ref. 19; the value of a_1 has been modified here to give zero thickness at the trailing edge. The latter airfoil is defined in Ref. 18 by a discrete distribution of points, from which the thickness distribution has been determined, and fit in a least-squares sense to the polynomial of Eq. (20). A family of uncambered airfoils, designated GK 70-10-XX, is developed by linearly scaling the resulting thickness function. The notation "XX" is the same here as before. The profile $y(x)$ for the two airfoils is obtained by scaling Eq. (20) by a thickness factor h , i.e., $y(x) = hf(x)$, where h represents the maximum thickness-to-chord ratio of the airfoil. The coefficients used in Eq. (20) to define the airfoils are given in Table 1.

Table 1 Airfoil coefficients

	NACA 00XX	GK 70-10-XX
a_0	1.4845	1.423840
a_1	-0.6405	-0.800726
a_2	-1.7580	0.141386
a_3	1.4215	-2.498820
a_4	-0.5075	1.734320

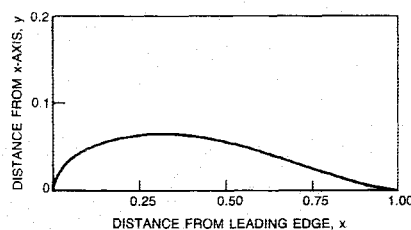


Fig. 2a Garabedian and Korn 70-10-13 airfoil thickness profile.

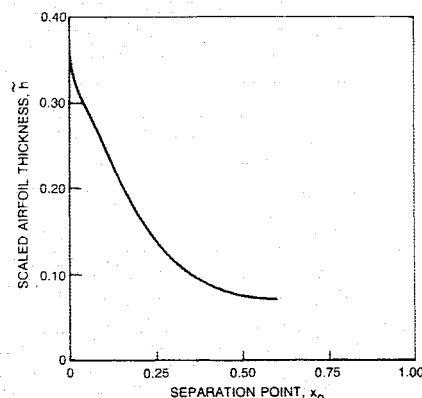


Fig. 2b Asymptotic behavior of separation point location for GK 70-10-XX airfoil.

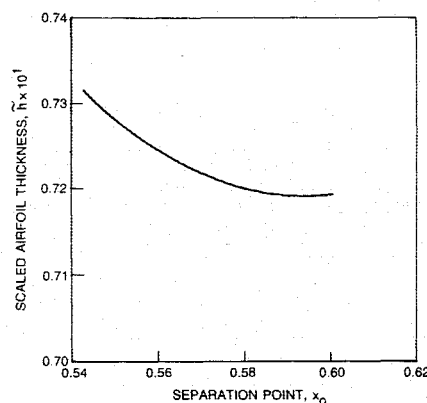


Fig. 2c Detail of asymptotic behavior of separation point location for GK 70-10-XX airfoil.

The laminar crossover behavior for the two airfoil families described has been determined using the triple-deck and the interacting boundary-layer analyses, and the results are given in the following sections. The finite Re calculations have been performed at a Reynolds number of 10^6 . The qualitative comparison between the results of the two analyses is discussed, with the predicted location of the separation point providing the basis of comparison. Using the interacting boundary-layer analysis, the effect of turbulence on the finite Reynolds number crossover process is also considered, through a study of the flow past two geometries—a NACA 00XX airfoil and a circular cylinder.

Triple-Deck Analysis

The triple-deck analysis has been used to determine the location of the separation point as the airfoil thickness is varied over a range beyond the critical value at which cutoff (wake inflation) occurs, i.e., for stalled airfoils. For this analysis, the airfoil thickness is scaled by the Reynolds number to yield a thickness parameter \bar{h} , given by the expression $\bar{h} = Re^{1/16} h$. Note that varying the thickness parameter is equivalent to varying the airfoil thickness at a fixed value of

Re , or perhaps more physically meaningful, it is equivalent to varying the Reynolds number for a fixed airfoil thickness h .

The result obtained for the NACA 00XX airfoil family is shown first. A representative profile is presented in Fig. 1a, namely, the NACA 0012 profile. The results are given in Fig. 1b in terms of the scaled thickness parameter \bar{h} . This airfoil has a wedge-shaped trailing edge and is free of inflection points; therefore, it is expected that the location of the separation point x_s , as a function of the airfoil thickness parameter, will be unique, based on the general predictions of triple-deck theory discussed earlier. As seen in Fig. 1b, the results agree with the expected behavior. As the airfoil thickness is decreased, the separation point moves aft toward the trailing edge. The curve terminates at the value of \bar{h} that corresponds to the collapse of the free streamline to the x axis at downstream infinity (cutoff).

The result obtained for the GK 70-10-XX airfoil family, for which the representative profile of the 13% thick airfoil is illustrated in Fig. 2a, is given in Figs. 2b and 2c. The profile shown in Fig. 2a displays the presence of an inflection point near the trailing edge, the existence of which introduces the possibility of nonuniqueness in the location of the separation point for a given value of the thickness parameter, as discussed. Nonuniqueness has been found to occur for the GK airfoil family, for which the separation point location is shown as a function of the airfoil thickness parameter in Fig. 2b. The nonuniqueness is not obvious on the scale of Fig. 2b, and although not pronounced, it is more apparent in the expanded view shown in Fig. 2c, which illustrates the behavior of the separation point location near the cutoff value of \bar{h} .

Interacting Boundary-Layer Analysis

The IBL analysis described earlier has been utilized to predict the way in which the flow undergoes crossover from local to massive separation, and to study the effect of turbulence upon crossover at finite Re . In addition to predicting the location of the separation point, this analysis allows local aerodynamic properties such as surface pressure and skin friction, as well as global properties such as drag, to be determined.

NACA 00XX Airfoil Family

Calculations have been performed for the NACA 00XX airfoil family using the LSI analysis, with the airfoil thickness systematically increased until the approach to cutoff (wake inflation) is observed. Following wake inflation, the MS analysis is applied as the airfoil thickness is further increased.

The predicted locations of the separation and reattachment points x_s and x_r , respectively, are shown in Fig. 3 as the airfoil thickness is varied. The approach of the reattachment point

curve to a horizontal tangent as h is increased signals the onset of wake inflation and the crossover from local to massive separation. In the present case, crossover occurs for a value of h between 0.06 and 0.07. Of particular importance to note in Fig. 3 is the apparently continuous behavior of the location of the separation point in going from the LSI to the MS model. This is consistent with the crossover behavior predicted by triple-deck theory for airfoils that are free of inflection points and have a wedge-shaped trailing edge, such as the NACA 00XX airfoil.

The effects of varying the airfoil thickness on the displacement body and the local aerodynamic properties, namely, the pressure coefficient C_p and the skin-friction coefficient C_f , are illustrated for the NACA 00XX airfoil family in Figs. 4a-c. In Fig. 4a, the airfoil profiles and the associated displacement

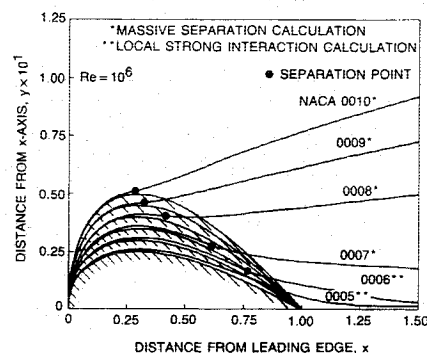


Fig. 4a Airfoil profile and displacement body for NACA 00XX airfoil.

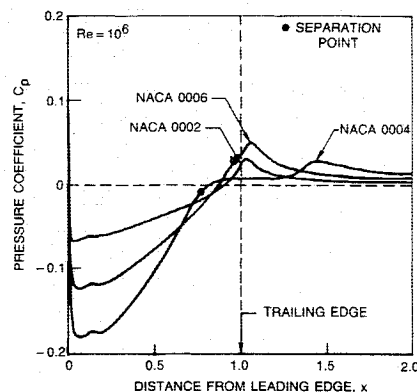


Fig. 4b Pressure distribution on airfoil surface and wake centerline for NACA 00XX airfoil using LSI method.

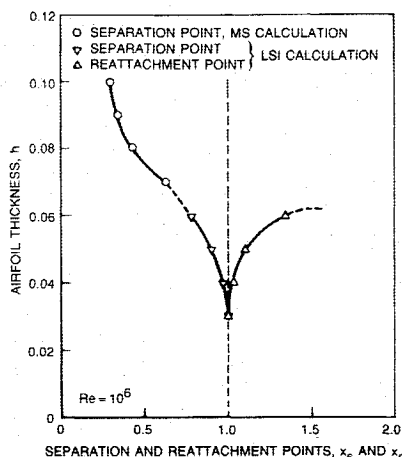


Fig. 3 Behavior of separation and reattachment point locations for NACA 00XX airfoil.

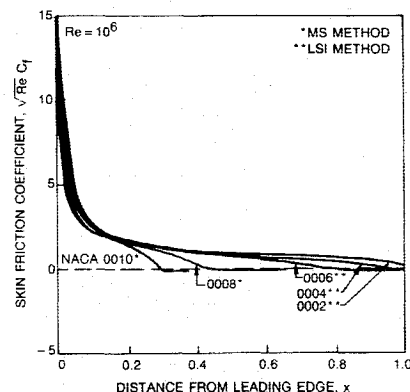


Fig. 4c Skin-friction distribution for NACA 00XX airfoil using LSI and MS methods.

bodies are plotted for various values of the thickness parameter h . The location of the separation point is also indicated in each case. First, note that as h increases, the displacement thickness increases, particularly in the vicinity of the trailing edge and in the downstream wake. As the value of h increases through the value at which wake inflation occurs, i.e., $0.06 < h < 0.07$, the length of the separated region undergoes a dramatic change, from $O(1)$ to a length on the order of the flow Reynolds number (according to the asymptotic theory⁸). Another observation is the tendency of the displacement body toward parabolic growth downstream, especially apparent for the NACA 0010 airfoil. The movement of the separation point toward the leading edge as h is increased is also clearly evident.

Figure 4b illustrates the behavior of the pressure coefficient C_p as the airfoil thickness is varied, calculated using the LSI analysis. The development of a distinct pressure plateau is seen as h is increased to a value of 0.06. Recall that the existence of a constant-pressure region downstream of the separation point is the fundamental feature assumed in applying the Kirchhoff eddy model to the massive separation calculations. The emergence of a constant-pressure region as the separation bubble grows is clearly demonstrated in the results obtained using the local strong interaction procedure; however, the plateau pressure $p_e \neq 0$. The behavior of the skin-friction coefficient C_f is shown in Fig. 4c. The development of an extensive separated flow region can be seen, with the separation point migrating toward the leading edge as the airfoil thickness is increased.

Garabedian and Korn 70-10-XX Airfoil Family

The results of the IBL analysis for the NACA 00XX airfoil family described have been found to be qualitatively consistent with the predictions of triple-deck theory. In particular, the crossover process is continuous for this airfoil. The possibility of discontinuous crossover (due to the existence of nonuniqueness) for certain types of airfoil profiles has been discussed earlier and has been shown to exist for airfoils with an inflection point in the vicinity of the trailing edge.¹⁰ In order to determine whether discontinuous behavior can be predicted at finite Reynolds numbers for a realistic airfoil, the Garabedian and Korn (GK) 70-10-XX airfoil family, for which discontinuous crossover is predicted by the triple-deck analysis, has been considered. The interacting boundary-layer analysis has been carried out in the same manner as previously described for the NACA 00XX series, and the results are presented in the following sections.

The locations of the separation and reattachment points are shown in Fig. 5. Following separation, which occurs on the GK airfoil at a value of $h \approx 0.05$, a very small increase in the airfoil thickness causes a considerable expansion of the separation bubble in the streamwise direction, in contrast to the slow initial growth of the bubble, which is observed for the NACA 00XX airfoil family after the boundary layer first separates. In particular, note the extremely large downstream change in the location of the eddy closure point that occurs between values of $h = 0.052$ and 0.053 for the GK airfoil family. A very important feature that can be seen in this figure is the absence of smooth merging between the two curves of x_s vs h obtained from the LSI and the MS analyses. This appears to be consistent with the qualitative prediction of triple-deck theory with respect to airfoils that have an inflection point near the trailing edge, like the GK airfoil.

The effects of varying the airfoil thickness upon the computed displacement body distributions and local aerodynamic properties, namely, the pressure coefficient and skin-friction coefficient, calculated for the GK airfoil family, will not be presented here, but can be found in Ref. 12.

Turbulence Effects

The effect of turbulence on the onset of massive separation has been studied as part of the present effort. Two geometries

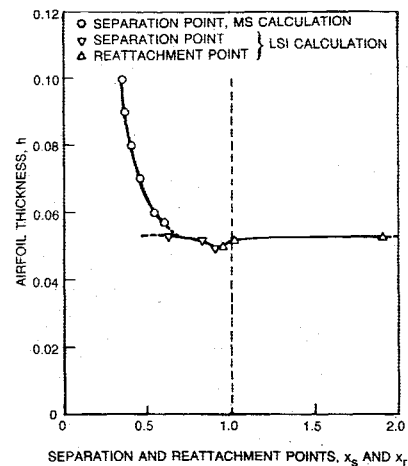


Fig. 5 Behavior of separation and reattachment point location for GK 70-10-XX airfoil.

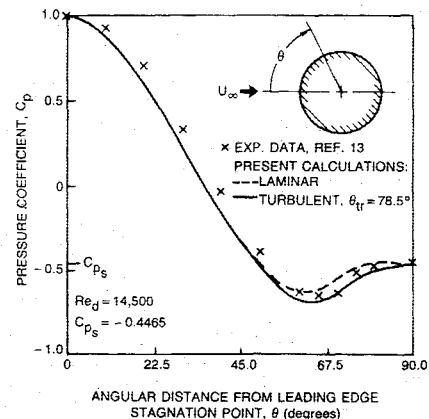


Fig. 6 Pressure distributions for laminar and transitional flow past circular cylinder with splitter plate, compared with experimental data.

have been considered, namely, the NACA 00XX airfoil and a circular cylinder with a trailing-edge splitter plate.

NACA 00XX Airfoil

The NACA 00XX series airfoil has been studied in an attempt to calculate the crossover between local and massive separation occurring in the presence of a turbulent boundary layer. Instantaneous transition to turbulent flow has been assumed to occur at a specified location on the airfoil surface. The present investigation into the effects of turbulence is only concerned with determining qualitative behavior; therefore, the transition location has been arbitrarily specified to be at $x = 0.35$ for all of the turbulent flow calculations.

The effect of turbulence has first been determined using the LSI analysis, with the airfoil thickness/chord ratio h varied to a maximum value of 14% at a Reynolds number of 10^6 . At the maximum thickness, the streamwise extent of the turbulent separation bubble is less than 1% of the chord, whereas for laminar flow at the same Re past the 6% thick airfoil, the extent of the separation bubble is approximately 60% of the chord. Since it is apparent that for $Re = 10^6$ the airfoil thickness has to be quite large to generate a significant turbulent separation bubble, an alternative means of inducing massive separation has been attempted, wherein the airfoil thickness is fixed and the Reynolds number has been varied. The effect of varying the Reynolds number on the extent of turbulent separation for the NACA 0014 airfoil has been considered. The locations of the separation and reattachment points have been determined as a function of the Reynolds

number, where transition to turbulence has been imposed at $x = 0.35$. The separation bubble is observed to shrink as the Reynolds number is increased for a fixed value of h ; the bubble vanishes between $Re = 1 \times 10^6$ and 2×10^6 . Both triple-deck theory and interacting boundary-layer theory predict the opposite trend for laminar flow, i.e., the laminar separation bubble grows as the Reynolds number is increased (e.g., see Figs. 1-3).

Although no massively separated turbulent flow solutions have been obtained for the NACA 00XX airfoil family over the ranges of h and Re considered, it is reasonable to expect that increasing the airfoil thickness until it is of $\mathcal{O}(1)$, i.e., until the airfoil becomes a bluff body, should induce massive separation. This expectation provides the motivation for the calculations of flow past a circular cylinder described next.

Circular Cylinder

In an effort to obtain a turbulent massively separated flow solution, the transitional flow past a circular cylinder has been calculated. The specific case considered is the flow past a cylinder with a downstream splitter plate at a Reynolds number (based on diameter) of 14,500, for which experimental data is available.²¹ A splitter-plate configuration has been chosen because the large-scale unsteadiness associated with vortex shedding is suppressed, making this data more suitable for comparison with the present steady-state numerical results than data obtained without a splitter plate.

The massive eddy present in a bluff-body flow is generally observed in experiments to be very nearly a constant-pressure region, where the pressure level is a function of the geometry and flow conditions. In the present massive separation model, the level of the pressure in the Kirchhoff eddy is a parameter that can be set; however, it can *not* be determined as part of the solution. Therefore, the results of the circular cylinder calculations currently presented have been obtained by specifying the eddy pressure to be the value measured experimentally; the specified value of the pressure coefficient is $C_p = -0.4465$.

An initial calculation has been performed assuming the flow to be completely laminar. The result of this calculation then has been used to determine the transition location for a subsequent turbulent calculation. The transitional calculation has been performed with instantaneous transition assumed to occur just aft of the location at which separation is predicted by the laminar calculation, at an angular distance θ of approximately 78.5 deg around the cylinder, measured from the forward stagnation point. The results of both calculations are presented in Fig. 6, along with the experimental data of Roshko.²⁰ Massive separation is predicted for both the laminar and the transitional flow. The two results are virtually identical until a value of θ of approximately 45 deg, after which a slightly lower pressure is predicted for the turbulent flow. Both pressure distributions are in good agreement with the experimental data.

The results of the preceding calculations lead to several important conclusions. The presence of a turbulent boundary layer, although it inhibits the initial onset of massive separation, does not prevent the occurrence of large-scale separated flow at finite Reynolds number. Also, results have been obtained that demonstrate that it is possible to compute bluff-body massive separation with the present IBL approach for massively separated flow. However, the eddy pressure cannot be obtained as part of the solution, but must be specified in order to achieve reasonable results. Finally, with the correctly specified value of the eddy pressure, good agreement with experimental data has been obtained, despite the fact that the present analysis has not been developed for application to bluff-body flows.

Concluding Remarks

The principal goal of the present study has been to initiate an investigation of the crossover process by which a flow with

small-scale local separation evolves into one with massive separation as airfoil thickness is increased. Two methods of analysis have been employed, one of which is based on triple-deck theory, which applies at the infinite Reynolds number asymptotic limit, and the second is based on interacting boundary-layer theory, and applies at finite Reynolds number.

An important result of the present investigation of crossover for realistic airfoils has been the demonstration that qualitative agreement exists between the results of the triple-deck and the interacting boundary-layer analyses. A consequence of the observed agreement is the recognition that the asymptotic theory can enhance the understanding of the crossover phenomenon predicted by finite Reynolds number methods of analysis. In addition, triple-deck theory provides the scalings that must be observed in generating mesh distributions for accurate numerical solutions of the finite Reynolds number crossover problem, regardless of the system of equations being solved. Since interacting boundary-layer theory provides efficient solutions even on fine meshes, an analysis like the one presented herein can be very helpful in providing guidance for the development of Navier-Stokes solution techniques for the investigation of massive separation and the crossover process and can provide a basis of comparison for the results of such analyses.

Most of the present results have been concerned with the crossover from local to massive separation for laminar flows. However, since most real boundary-layer flows are turbulent over at least a portion of the airfoil surface, turbulence has been introduced in the interacting boundary-layer analysis. As expected, turbulence has been observed to strongly inhibit the initial onset of separation, thereby delaying stall considerably in comparison with a completely laminar flow. The extent of turbulent separation has been found to decrease as the Reynolds number is increased, which is opposite to the trend observed for laminar separation. In addition, the massively separated flow past a bluff body, namely, a circular cylinder with a trailing-edge splitter plate, has been calculated using the present finite Reynolds number analysis. Both the laminar and transitional flow results agree well with the experimentally measured pressure distribution, provided the correct eddy pressure is specified.

The principal conclusion of this study is that the interacting boundary-layer approach is a useful and efficient method for the prediction of small- and large-scale boundary-layer separation on airfoils, and thus provides a potential vehicle for the comprehensive analysis of airfoil performance. Several aspects of the present technique should be pursued in the future in order to permit the analysis of a broader range of problems than can currently be addressed and to allow more accurate modeling of the physical processes occurring in separated flows. Two areas that should be considered in future work are discussed in the next paragraph.

The Kirchhoff eddy model used here leads to a reasonable massive separation model for the local body-scale flow but does not provide a means for predicting the constant-pressure level in the eddy, which currently has to be assumed or obtained from experimental data. It is evident that a better model for the eddy, in particular, one that would allow the eddy pressure to be determined as part of the solution, should be pursued. In order to determine the eddy pressure, the downstream structure of the eddy, particularly in the closure region, will have to be accounted for. The recently introduced analysis of Rothmayer²¹ takes an important step in this direction, allowing the efficient calculation of the complete eddy structure, including closure, free of the assumptions of the Kirchhoff eddy model. Another suggested area for future research is in the development of the capability of treating lifting airfoils. The present study has been limited to nonlifting airfoils, while the operation of real airfoils, and particularly the occurrence of massive separation, is often associated with nonsymmetric geometries and/or high angle-of-attack flight conditions.

Acknowledgments

This work was supported by NASA Langley Research Center Contract NAS1-16585. The author gratefully acknowledges Drs. M. J. Werle and J. E. Carter of UTRC and Profs. A. P. Rothmayer of Iowa State University and F. T. Smith of University College, London, for their many helpful discussions during the course of this study. Thanks are also due to Dr. J. M. Verdon of UTRC for his helpful suggestions during the preparation of this manuscript.

References

- ¹Sychev, V. V., "On Laminar Separation," *Mekhanika Zhidkosti i Gaza*, No. 3, May-June 1972, pp. 47-59.
- ²Smith, F. T., "The Laminar Separation of an Incompressible Fluid Streaming Past a Smooth Surface," *Proceedings of the Royal Society of London*, Series A, Vol. 356, 1977, pp. 443-463.
- ³Smith, F. T., "A Structure for Laminar Flow Past a Bluff Body at High Reynolds Number," *Journal Fluid Mechanics*, Vol. 155, June 1985, pp. 175-191.
- ⁴Cheng, H. K. and Rott, N., "Generalizations of the Inversion Formula of Thin Airfoil Theory," *Journal of Rational Mechanics and Analysis*, Vol. 3, May 1954, pp. 357-382.
- ⁵Rothmayer, A. P. and Davis, R. T., "Massive Separation and Dynamic Stall on a Cusped Trailing-Edge Airfoil," *Numerical and Physical Aspects of Aerodynamic Flows III*, edited by T. Cebeci, Springer-Verlag, New York, 1986, pp. 286-317.
- ⁶Smith, F. T., "Laminar Flow of an Incompressible Fluid Past a Bluff Body: The Separation, Reattachment, Eddy Properties and Drag," *Journal Fluid Mechanics*, Vol. 92, Pt. 1, 1979, pp. 171-205.
- ⁷Smith, F. T., "Nonuniqueness in Wakes and Boundary Layers," United Technologies Research Center, East Hartford, CT, Rept. UTRC83-15, May 1983.
- ⁸Cheng, H. K. and Smith, F. T., "The Influence of Airfoil Thickness and Reynolds Number on Separation," *Journal Applied Mathematics and Physics (ZAMP)*, Vol. 33, March 1982, pp. 151-180.
- ⁹Kirchhoff, G., "Zur Theorie freier Flüssigkeitsstrahlen," *Journal für die reine und angewandte Mathematik* Vol. 70, 1869, p. 289.
- ¹⁰Rothmayer, A. P., "A Study of High Reynolds Number Laminar Separation," Ph.D. Dissertation, Univ. of Cincinnati, Dept. of Aerospace Engineering and Engineering Mechanics, May 1985.
- ¹¹Werle, M. J. and Verdon, J. M., "Viscid/Inviscid Interaction Analysis for Symmetric Trailing Edges," United Technologies Research Center, East Hartford, CT, Rept. R79-914493-5, 1980.
- ¹²Barnett, M. and Carter, J. E., "An Analysis of the Crossover Between Local and Massive Separation on Airfoils," NASA Contractor Rept. 4096, Sept. 1987.
- ¹³Cebeci, T. and Smith, A. M. O., *Analysis of Turbulent Boundary Layers*, Academic Press, New York, 1974.
- ¹⁴Chang, K. C., Bui, M. N., Cebeci, T., and Whitelaw, J. H., "The Calculation of Turbulent Wakes," *AIAA Journal*, Vol. 24, Feb. 1986, pp. 200-201.
- ¹⁵Ashley, H. and Landahl, M., *Aerodynamics of Wings and Bodies*, Addison-Wesley, Reading, MA, 1965.
- ¹⁶Veldman, A. E. P., "A Calculation Method for Incompressible Boundary Layers with Strong Viscous-Inviscid Interaction," NLR MP 79029 U, presented at 3rd GAMM Conference on Numerical Methods in Fluid Mechanics, Oct. 10-12, 1979, Kolm, W. Germany.
- ¹⁷Davis, R. T. and Werle, M. J., "Progress on Interacting Boundary-Layer Computations at High Reynolds Number," *Numerical and Physical Aspects of Aerodynamic Flows*, Springer-Verlag, New York, 1982, pp. 187-210.
- ¹⁸Bauer, F., Garabedian, P., Korn, D., and Jameson, A., "Supercritical Wing Sections II," *Lecture Notes in Economics and Mathematical Systems*, Vol. 108, Springer-Verlag, Berlin, 1975.
- ¹⁹Abbott, I. H. and von Doenhoff, A. E., *Theory of Wing Sections*, Dover, New York, 1959.
- ²⁰Roshko, A., "On the Drag and Shedding Frequency of Two-Dimensional Bluff Bodies," NACA TN 3169, July 1954.
- ²¹Rothmayer, A. P., "The Calculation of Laminar Separation Bubbles in the Wake Inflation/Deflation Regime," AIAA Paper 88-0605, Jan. 1988.